ACADEMIC PRESS

Available online at www.sciencedirect.com

SCIENCE DIRECT®

Journal of Solid State Chemistry 171 (2003) 349–352

JOURNAL OF SOLID STATE CHEMISTRY

http://elsevier.com/locate/jssc

Selective spin-state and metal–insulator transitions in $GdBaCo_2O_{5.5}$

C. Frontera,[a,*] J.L. García-Muñoz,[a] A. Llobet,[b] Ll. Mañosa,[c] and M.A.G. Aranda[d]

[a] *Institut de Ciència de Materials de Barcelona, CSIC, Campus Universitari de Bellaterra, E-08193 Bellaterra, Spain*
[b] *Laboratoire de Magnetisme Louis Néel, CNRS 25 Avenue des Martyrs - BP 166, 38042 Grenoble Cedex 9, France*
[c] *Dep. d'Estructura i Constituents de la Matèria, Facultat de Física, Universitat de Barcelona, E-08028 Barcelona, Spain*
[d] *Departamento de Química Inorgánica, Cristalografía y Mineralogía Universidad de Málaga, E-29071 Málaga, Spain*

Received 6 May 2002; received in revised form 25 July 2002; accepted 31 July 2002

Abstract

By means of ultra-high resolution synchrotron diffraction and calorimetry measurements we have studied the metal–insulator transition in $GdBaCo_2O_{5.5}$. The appearance of the metallic state is attributed to a sudden excitation of some electrons in the octahedra (t_{2g}^6 state) into the Co e_g band (final $t_{2g}^4e_g^2$ state). In contrast, the $t_{2g}^5e_g^1$ state in the pyramids does not change at the transition. Calorimetry measurements show that the insulator-to-metal transition is first order and the entropy change estimated from the latent heat corroborates the pictured scheme.

Cobalt oxides with perovskite structure have demonstrated to be a very challenging family of compounds. In addition to the strong spin–charge–lattice correlations present in Cu and Mn oxides, the spin-state degree of freedom of Co ions introduces new effects in these narrow band oxides [1,2]. Co^{3+} ions can present three different spin states: the low spin state (LS, $t_{2g}^6e_g^0$), the intermediate spin state (IS, $t_{2g}^5e_g^1$), and the high spin state (HS, $t_{2g}^4e_g^2$). HS (LS) is associated with values of crystal field (CF) smaller (larger) than the intra-atomic exchange energy. The IS state appears when similar values of these two energies are combined with the electron–phonon coupling and the Jahn–Teller distortion that lifts the degeneracy of e_g and t_{2g} orbitals. In many cobaltites the energy differences between spin states are small and can be easily overcome by thermal fluctuations and/or changed by the lattice thermal evolution [2] leading to spin-state transitions. The size of Co^{3+} ions depends on its spin state, and anomalous cell volume changes have been found at the spin state transitions in $LaCoO_3$ [2].

More recently, a great interest on $LnBaCo_2O_{5+\delta}$ ($Ln \equiv$ rare earth) cobaltites has appeared [3–10]. This family of compounds presents spin-state transitions [6,9,10], charge ordering [7,8], and giant magnetoresistance [4,10]. The oxygen content δ ($0 \leqslant \delta \leqslant 1$) controls the nominal valence of Co ions that varies from 3.5+ (50% of Co^{3+} and 50% of Co^{4+}) for $\delta = 1$ to 2.5+ (50% of Co^{3+} and 50% of Co^{2+}) for $\delta = 0$ passing through 100% of Co^{3+} for $\delta = 0.5$. These compounds present a high degree of order. Ba and *Ln* order forming (0 0 1) layers alternating in the *c* direction. In addition, the oxygen vacancies (when $\delta < 1$) are placed in the layers of the rare earth ions. Thus, these compounds are formed by the stacking sequence $[CoO_2][BaO][CoO_2][LnO_\delta]$ along the *c* direction, leading to the coexistence of two types of Co-coordination environments: pyramidal CoO_5 and octahedral CoO_6. Moreover, oxygen vacancies, within the $[LnO_\delta]$ layers, present a strong tendency to order. For $\delta = 0.5$ the oxygen atoms and vacancies are located in alternating rows [5,9]. This order prevents the randomness in the magnetic superexchange interactions that causes spin glass behavior in oxygen-deficient $La_{1-x}Sr_xCoO_{3-\varepsilon}$ compounds.

A metal–insulator (MI) transition is present in several $LnBaCo_2O_{5.5}$ compounds [5]. Susceptibility measurements reveal that coinciding with this transition there is a large change in the effective paramagnetic moment of the samples. This is understood as a sudden increase, on heating, in the spin state of Co ions [5,9,10]. From magnetic measurements on several samples with different lanthanides, all displaying the MI transition, Maignan et al. [5] suggested a coexistence of IS (pyramids) and LS (octahedra) for $T < T_{MI}$ and HS Co^{3+} at high enough temperatures. Nevertheless, the

*Corresponding author.
E-mail address: frontera@icmab.es (C. Frontera).

0022-4596/03/$ - see front matter © 2003 Elsevier Science (USA). All rights reserved.
doi:10.1016/S0022-4596(02)00232-3

spin state at both sides of the MI transition is still unclear. A study of the structural changes was carried out for $TbBaCo_2O_{5.5}$ by Moritomo et al. [9]. Based on these structural data, they proposed a spin-state transition from a full IS state scheme to the HS state (for $Ln = Tb$) in both pyramidal and octahedral sites [9]. For $T > T_{MI}$ a HS state [5,9] and a coexistence of HS/IS states have been proposed [10] by different groups. The main conclusion of Moritomo et al. is that the orbital degree of freedom of the IS state ($t_{2g}^5 e_g^1$) and the electron–phonon coupling results in a Jahn–Teller cooperative distortion and a $d_{3x^2-r^2}/d_{3y^2-r^2}$-type orbital order (OO) below T_{MI}. As the origin of the transition they proposed a sudden distortion of the basal planes, on cooling, that accommodate the $d_{3x^2-r^2}$ (pyramid) and $d_{3y^2-r^2}$ (octahedron) orbital occupancy [9]. However, the sample studied in Ref. [9] had impurities and the reported errors in the Co–O distances were anomalously large.

We have studied a polycrystalline sample of $GdBaCo_2O_{5+\delta}$. It was prepared by standard solid-state reaction in air as has been previously reported [10]. We have characterized the structural evolution across the MI transition using X-ray thermodiffractometry (Gd has a very high neutron absorption coefficient). Ultra-high resolution synchrotron X-ray powder diffraction (SXRPD) patterns were collected at BM16 diffractometer of ESRF (Grenoble) in the standard Debye–Scherrer configuration. Measurements have been done at $T = 300$, 320, 340, 360, 380 and 400 K. The powder patterns were analyzed by the Rietveld method using the GSAS suite of programs [11]. No impurities peaks have been detected and the diffraction peaks were remarkably sharp for a three metal-containing perovskite. This warrants the good quality of the studied sample. The oxygen stoichiometry was determined to be 5.53(1) from SXRPD data, a usual oxygen content found for air-synthesis [5,9]. Moreover, according to Ref. [5] the MI transition is absent in Gd samples with $\delta \geqslant 0.6$. Differential scanning calorimetry (DSC) measurements have been taken in a TA-Instruments commercial calorimeter (model 2920) using a temperature ramp of 5 K/min.

The structure of $TbBaCo_2O_{5.5}$ reported in Ref. [9], with $P\,mmm$ space group with $a \simeq a_p$, $b \simeq c \simeq 2a_p$ ($a_p \equiv$ primitive perovskite lattice parameter), was used as starting model for the Rietveld refinements. The oxygen vacancies were checked in our $GdBaCo_2O_{5.5}$ sample and found to be located at the lanthanide layers in such a way that CoO_6 octahedra form (010) layers alternated along the b-axis with (010) layers of corner-sharing CoO_5 square pyramids, as in $TbBaCo_2O_{5.5}$. R_F agreement factor ranges between 3.91% ($T = 300$ K) and 4.36% ($T = 400$ K). Refined atomic coordinates will be published elsewhere. On cooling through the transition, b and c lattice parameters exhibit a sudden shrink (0.28 and 0.27%, respectively) while a lengthens at T_{MI} (0.35%), see Fig. 1(a). This contrasts with the results reported for $TbBaCo_2O_{5.5}$ [9]. Figs. 1(b) and (c) show the Co–O bond distances, for CoO_6 octahedron and CoO_5 pyramid respectively, along the three crystallographic axes (Co–Oi stands for bond lengths along $i = a$-, b- and c-axis). There are also important differences with the case of $TbBaCo_2O_{5.5}$ [9]. We have found that pyramids and octahedra are deformed in both the insulating and metallic states. The longest Co–O distance is Co–Oa for the former (CoO_5) and Co–Ob for the latter (CoO_6). Long and short bonds alternate along the b-axis at both sides of the transition. This is well different from the evolution reported in Ref. [9] for $TbBaCo_2O_{5.5}$, where that alternation was only clearly observed below T_{MI} and it was stated that the basal plane deformation in pyramids and octahedra vanishes above T_{MI}. Conversely with Ref. [9], our data discard the stabilization of a $d_{3x^2-r^2}/d_{3y^2-r^2}$-type OO below T_{MI} as the physical mechanism for the MI transition in $GdBaCo_2O_{5.5}$: we show in Figs. 1(b) and (c) that the difference between long and short Co–O bonds in the basal plane (the Q_2-type antiferrodistorsive distortion) remains practically unchanged in the pyramid and increases strongly in the octahedron when heating above T_{MI}.

Fig. 1(d) shows the temperature dependence of the inverse susceptibility in the paramagnetic region up to 625 K. As discussed in Ref. [10] the values of the effective magnetic moment obtained below and above T_{MI} suggest that the spin state of Co^{3+} is a 1:1 mixture of LS/IS and a 1:1 mixture of HS/IS, respectively. Since IS Co^{3+} is most probable in the pyramids [5,12], the results indicate that, below T_{MI}, the octahedron contains LS Co^{3+} and the pyramid IS Co^{3+}.

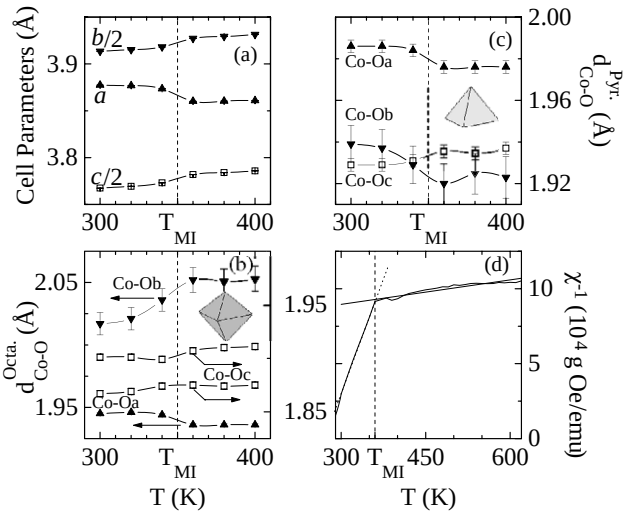

Fig. 1. Temperature dependence of (a) lattice constants; (b) Co–O bond distances for the CoO_6 octahedra (Co–Oi stands for the bond lengths along $i = a$-, b- and c-axis); (c) Co–Oi bond distances for the CoO_5 pyramids; and (d) inverse of the susceptibility χ_{Co} (the straight lines show the Curie fits above and below T_{MI}).

Fig. 2(a) and (b) show the (underlying) heat flow obtained by DSC during heating and cooling, respectively. The hysteresis in the cooling and heating processes evidences that the transition is first order. Fig. 2(c) shows the thermal evolution of dq/dT. The latent heat and entropy change, during the transition, estimated from this curve are $\Delta h = 8.155$ kJ/mol and $\Delta s = 2.73R$.

Let us now analyze in more detail the Co–O bond length variation. As shown in Figs. 1(b) and (c), the apical Co–O*c* distances of the octahedron and pyramid changes little across the transition. Co–O*a* and Co–O*b* basal distances of the pyramid both lengthen on cooling, in a so similar way that the basal plane deformation remains practically unchanged at both sides of T_{MI}. This is not compatible with the stabilization of $d_{3x^2-r^2}$-type OO in the insulating phase. In contrast the Co–O*b* distance in the octahedra displays a pronounced shrinking on cooling, which is accompanied by a moderate increase of the Co–O*a* distance. As a result, the basal distortion decreases notably on cooling through T_{MI}, the opposite of that one would expect for the stabilization of $d_{3y^2-r^2}$-type OO below T_{MI}. At this point it is important to recall that a transition to a higher spin state in Co^{3+} (as deduced from magnetic data) implies a bigger effective ionic radius which should lengthen the average $\langle d_{Co-O} \rangle$ bond length. Fig. 3(a) shows the evolution of $\langle d_{Co-O} \rangle$. A very significant finding is the different evolution of this distance in the octahedron and the pyramid: $\langle d_{Co-O} \rangle$ distance of the octahedron increases substantially at T_{MI} on heating but that of pyramid decreases. This finding constitutes the first experimental result establishing that the spin-state transition in $LnBaCo_2O_{5.5}$ occurs solely in the octahedra. Thus, in the pyramids we observe, on heating, the metal–oxygen bond-length contraction normally found when the gap closes and enters the metallic phase. This spin-state change is also responsible

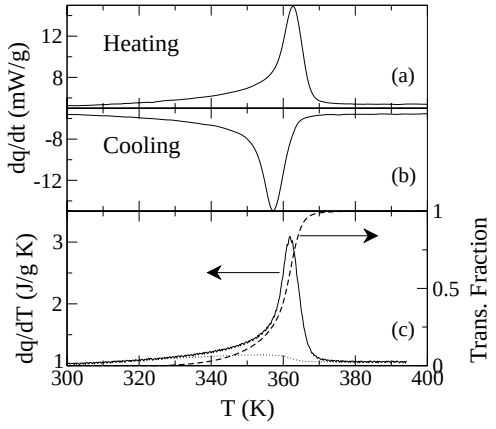

Fig. 2. Heat flow vs. temperature on heating (a) and on cooling (b) with a rate of ± 5 K/min. Panel (c) shows the flow dq/dT in the heating process (left axis) together with the baseline (dotted line) used for the integration of the peak, and the evolution of the fraction transformed (right axis, dashed line) obtained.

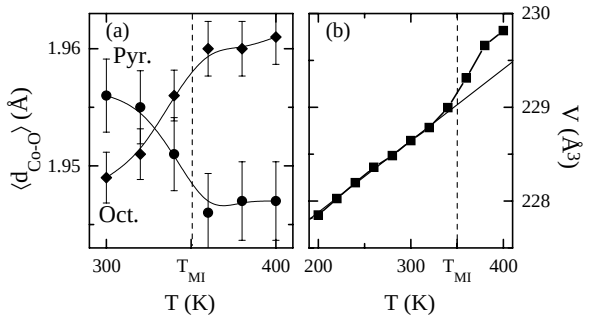

Fig. 3. Temperature dependence of (a) average Co–O distances for the CoO_6 and CoO_5 polyhedra and (b) unite cell volume. The continuous straight line in (b) is a guide-to-the-eyes to highlight the anomalous volume expansion at T_{MI}.

for the anomalous volume expansion at T_{MI} plotted in Fig. 3(b). Normally, the cell volume contracts in an electron delocalization process but expands in a transition to a higher spin state [2].

The entropy change found by means of DSC confirms this picture. The LS state of Co^{3+} is non-degenerated ($g_{LS} = 1$), while the degeneracy of the HS state is $g_{HS} = 15$ [13]. Thus, the expected entropy change due to the larger degeneracy of the HS is $\Delta s = R \ln g_{HS}/g_{LS} \simeq 2.71R$ in complete agreement with the value found ($2.73R$).

In summary, from the analysis of structural changes, magnetic behavior and entropy change during the MI transition for $GdBaCo_2O_{5.5}$ we can conclude that: (i) There is a sudden expansion of $\langle d_{Co-O} \rangle$ distance of octahedra at T_{MI}, concomitant with a first-order spin-state transition from LS (insulating) to HS (metallic) state in the Co^{3+} ions of the octahedra. (ii) Co atoms in the pyramids hold the same spin state (Co^{3+} IS) before and after the electronic delocalization. Hence, the pyramid simply shrinks as commonly observed in Mott oxides when they enter the metallic phase. (iii) The alternation of short and long Co–O bonds along the *b*-axis is present in the insulating and the metallic phases. The Q_2-type distortion (antiferrodistorsive) of the basal planes does not increase in the insulating phase, ruling out a $d_{3x^2-r^2}/d_{3y^2-r^2}$-type OO as the origin of the transition. So, the driving force for the MI transition is a spin-state change in the Co^{3+} ions located at the octahedra, which suddenly switch from LS ($t_{2g}^6 e_g^0$) to HS ($t_{2g}^4 e_g^2$) state at T_{MI}. Thereby, the metallic conductivity in this family of oxides (full Co^{3+}) seems related with the injection of electrons in the conduction band that accompanies this transition.

Financial support by the MEC (PB97-1175), CICyT (MAT97-0699, MAT97-326-C4-4, and MAT99-0984-C03-01) and Generalitat de Catalunya (GRQ95-8029) projects is thanked. C.F. acknowledges financial support from MCyT (Ramón y Cajal program). ESRF is acknowledged for the provision of X-ray synchrotron

facilities and Dr. E. Dooryee for his assistance during data collection.

References

[1] G. Thornton, et al., J. Solid State Chem. 61 (1986) 301;
M.A. Señaris-Rodríguez, J.B. Goodenough, J. Solid State Chem. 116 (1995) 224;
W.C. Koehler, E.O. Wollan, J. Phys. Chem. Solids 2 (1957) 100;
J.B. Goodenough, J. Phys. Chem. Solids 6 (1958) 287;
M. Zhuang, et al., Phys. Rev. B 57 (1998) 10705;
T. Saitoh, et al., Phys. Rev. B 55 (1997) 4257;
S. Yamaguchi, et al., Phys. Rev. B 55 (1997) R8666;
M.A. Korotin, et al., Phys. Rev. B 54 (1996) 5309.
[2] K. Asai, et al., J. Phys. Soc. Jpn. 67 (1998) 290.
[3] W. Zhoug, et al., Adv. Mater. 5 (1993) 735;
W. Zhou, Chem. Mater. 6 (1994) 441;
C. Martin, et al., Appl. Phys. Lett. 71 (1997) 1421;
Y. Moritomo, et al., Phys. Rev. B 58 (1998) R13334.
[4] I.O. Troyanchuk, et al., Phys. Rev. Lett. 80 (1998) 3380;
I.O. Troyanchuk, et al., Phys. Rev. B 58 (1998) 2418.
[5] A. Maignan, et al., J. Solid State Chem. 142 (1999) 247.
[6] E. Suard, et al., Physica B 276–278 (2000) 254.
[7] T. Vogt, et al., Phys. Rev. Lett. 84 (2000) 2969.
[8] E. Suard, et al., Phys. Rev. B 61 (2000) R11871.
[9] Y. Moritomo, et al., Phys. Rev. B 61 (2000) R13325.
[10] M. Respaud, et al., Phys. Rev. B 64 (2001) 214401.
[11] A.C. Larson, R.B. Von Dreele, Los Alamos National Lab. Rep. No. LA-UR-86-748, 1994.
[12] S.K. Kwon, et al., Phys. Rev. B 62 (2000) R14637.
[13] W. Koshibae, et al., Phys. Rev. B 62 (2000) 6869.